For World Scientific Publishing
CO PTE LTD
ANL-HEP-PR-88-13

E-581/704

POLARIZED-PROTON AND-ANTIPROTON BEAMS AT FERMILAB AND ASSOCIATED EXPERIMENTS§

Akihiko Yokosawa

High Energy Physics Division
Argonne National Laboratory, Argonne, Illinois

12 April 1988

We describe the polarized-proton and-antiproton beams up to 200 GeV/c in the Fermilab MP beam line which is currently operational. We also present the Fermilab polarized-beam program using this facility. These Fermilab polarization projects are designated as E-581/704 initiated and carried out by an international collaboration, Argonne (U.S.), Fermilab (U.S.), Kyoto (Japan), LAPP (France), Northwestern University (U.S.), Los Alamos Laboratory (U.S.), Rice (U.S.), Saclay (France), Serpukhov (U.S.S.R.), INFN Trieste (Italy), and University of Texas (U.S.).

1) INTRODUCTION

Ever since polarized beams and/or polarized-proton targets became available for the use of high-energy experiments, various measurements on the polarization phenomena have been extensively carried out. Asymmetry measurements are sensitive to interference terms between dominant and non-dominant amplitudes, and thus provide useful information which can not be obtained from differential cross-section measurements alone, on the study of production and reaction mechanisms.

§ Work supported by the U.S. Department of Energy, Division of High Energy Physics, Contract W-31-109-ENG-38.

The submitted manuscript has been authored by a contractor of the U. S. Government under contract No. W-31-109-ENG-38. Accordingly, the U. S. Government retains a nonexclusive, royalty-free license to publish or reproduce the published form of this contribution, or allow others to do so, for U. S. Government purposes.

The physics objectives for the Fermilab polarized-beam facility up to 200 GeV/c are in part based upon the facts that there are already several experimental indications that spin effects are significant at high energy. They are i) measurements of π^0 production at high $p_\perp (p_\perp > 2.0$ GeV/c) in proton-proton at CERN and in π^--proton collisions at Serpukhov revealed sizeable asymmetries at 24 GeV/c and 40 GeV/c, respectively ii) hyperons produced at large x_F inclusively off nuclei and hydrogen at CERN, Fermilab, and ISR, were observed to have high polarizations iii) inelastic scattering of longitudinally polarized electrons on longitudinally polarized protons at SLAC yielded a large asymmetry, implying that proton helicity orientation is communicated to the constituent quarks. Thus, spin dependence in quark-quark collisions can be inferred from measurements of spin dependence in proton-proton collisions in appropriate kinematic regions.

The observation of these large effects suggests that the underlying processes involved might be simple at the level of constituents. A number of theoretical models have been introduced to explain these polarization phenomena and predictions for future measurements have been made.

2) FERMILAB POLARIZED-BEAM (protons and anti-protons) FACILITY AND COMMISSIONING OF THE POLARIZED BEAM (E-581)

During the last decade, construction of a high-energy (above 100 GeV/c) polarized beam has been attempted. In order to avoid possible complications involving depolarization at high energies, polarized protons can be produced from decaying hyperons, lambdas or sigmas. The Fermilab polarized-beam facility was constructed and has been operational during the last TeV-II (fixed target) period which ended 15 February 1988.

Design and Construction of Polarized Beam

A polarized proton beam from Λ^0 decay at Fermilab has been suggested by Overseth[1] in 1969 applying the fact that the protons from lambda decay are polarized along their direction of motion in the lambda rest frame. This polarization has been measured by Cronin and Overseth[2] to determine the relative amounts of s wave and p wave in the decay. For unpolarized lambdas, the polarization of the proton in the direction of the proton is $\alpha = 0.64$, where

$$\alpha = 2\,\mathrm{Re}|s \cdot p^*|/(|s|^2 + |p|^2),$$

and s and p are the s wave and p wave amplitudes in the parity violating decay.

Since then more detailed work has been carried out at CERN.[3] The idea then was to select high-momentum protons which were forward decaying, around $\theta_{c.m.} = 0°$, from lambdas near the highest momentum point of the lambda-production spectrum. These protons were longitudinally polarized and therefore would have many rotations of the spin prior to reaching a final focal point. We note that this method could not be applied to protons with much lower momentum than the incident energy.

It has been shown that we can select protons or antiprotons at various momenta which are decaying around $\theta_{c.m.} = 90°$ from lambdas or antilambdas respectively.[4] We show how this scheme works.

The spin direction in the lambda center-of-mass (decay frame) is shown in Fig. 1. We note that spin direction is almost unchanged in transforming from the lambda-decay frame to the laboratory. Therefore protons or antiprotons decaying around $\theta_{c.m.} = 0°$ and 180° are longitudinally polarized ($\vec{L}$) while

those with $\theta_{c.m.} = \pm 90°$ are transversely polarized ($\vec{N}$, up and down, or $\vec{S} = \vec{N} \times \vec{L}$) in the laboratory.

Protons or antiprotons with $\theta_{c.m.} = 90°$ and $-90°$ have the opposite laboratory decay angles which are not zero. They can be distinguished from those decaying at $\theta_{c.m.} = 0°$ from lambda or antilambda with the production target as the source of the beam. Virtual sources for $|\theta_{c.m.}| = 90°$ particles are illustrated in Fig. 2. The spin direction, $\vec{N}$ or $\vec{S}$, should be chosen using the field direction of the sweeping magnets and bending magnets for the momentum selection, so that the spin direction is parallel to the field. The polarized beam line designated as MP is located in the meson area as shown in Fig. 3 and it consists of the MP primary beam and MP secondary beam. The primary beam line is shown in Fig. 4, where a parasitic target (MP2TGT) is typically used to produce an electron beam for calibration purposes. The secondary beam line up to 200 GeV/c is shown in Fig. 5. Here we produce the $\vec{S}$ type beam before reaching the snake magnets which make fast reversal, typically every 10 spills, of the spin direction.[5] The snake magnets consisting of twelve dipoles with 45° precessions as shown in Fig. 6 can also change the spin direction from $\vec{S}$ to $\vec{N}$ or $\vec{S}$ to $\vec{L}$ without altering beam direction and phase space before and after the magnets. These magnets are expected to control systematic errors by periodic reversal.

Polarized protons from the virtual sources as shown in Fig. 2 are focused in the tagging section, where both the momentum and polarization are selected (see Fig. 5). The polarization is strongly related to the x position (x, y, z directions are indicated in Fig. 5) at the tagging section, and the average polarization, $\langle P \rangle$, and $I\langle P \rangle^2$, where I represents actually measured beam intensity, are shown in Figs. 7 and 8 respectively with respect to x in mm. The estimated intensities of polarized beams with a beam polarization of 45% pro-

duced by 400-GeV/c and 1000-GeV/c incident protons are shown in Fig. 9. The momentum and flux of the present polarized-beam line are limited by the quadrupole strength. We are proposing to upgrade the present conventional quads to 4" superconducting quads. The estimated flux are shown in Fig. 10.

The beam line was actually operated at 800-GeV/c incident momentum. The intensities of total (not tagged) protons and antiprotons at 200 GeV/c were $1.5 \cdot 10^7$/spill and $1.5 \cdot 10^6$/spill respectively for incident protons with 10^{12}/spill. The intensities of tagged polarized beams with polarization higher than 40% will soon be available. Two polarimeters were utilized to determine the polarization of the polarized beams. We describe these polarimeters currently installed in the experimental hall.

1) Coulomb-Nuclear Polarimeter

Several authors since Schwinger[6] have indicated non zero polarization in the Coulomb-nuclear interference region in nucleon-nucleon scattering. This polarimeter is to measure the interference term of the non-flip amplitude and the electromagnetic spin-flip amplitude. The proton polarization arising from the interference is $P \approx 5\%$ at $|t| \approx 2 \cdot 10^{-3}$ $(\mathrm{GeV/c})^2$ and is energy independent.[7]

For a beam momentum of 200 GeV/c, we operate the C-N polarimeter covering $0.1 < \theta_{lab} < 0.5$ mrad. Such scattering angles are smaller than the beam divergence (~ 1 mrad) so that kinematic overdetermination becomes imperative for adequate background suppression. We utilize a forward spectrometer consisting of the BM-109 magnet and MWPC's (multiwire proportional chamber) as shown in Fig. 11. The recoil protons with energies from 0.5 to 5 MeV will also be detected by scintillation targets.

2) Primakoff-Effect Polarimeter

The diffractive dissociation of incoming high-energy proton into (πN) system by the Coulomb field of nuclei[8] is related to the low-energy photoproduction including the polarization effect.[9] This fact can be applicable to a polarimeter for high-energy polarized beams.[10] The process $pA \rightarrow pA\pi^\circ$ can be related via the Primakoff effect to low-energy photoproduction, i.e., $\gamma p \rightarrow \pi^\circ p$. The amplitude ψ for diffractive production from a nucleus with charge Z and atomic number A can be written as:[9]

$$\int |\psi|^2 \, d\phi = \frac{Z^2\alpha}{p_\perp^2} \left(\frac{2M_A}{s_{\pi p} - m_p^2}\right)^2 \left(A \cdot \frac{d\sigma}{d\Omega}\right)_{\gamma p \rightarrow \pi^0 p},$$

where A is the photoproduction asymmetry at the given value of $p_\perp$ and $s_{\pi p}$. Results of measurements in $\gamma p^\uparrow \rightarrow \pi^\circ p$ at the γp kinetic energy of 600 MeV show that the photoproduction asymmetry is $\sim 90\%$ at $\theta_{c.m.} \approx 90^\circ$ and $m_{p\pi^\circ} = 1.4$ GeV/c^2. The scheme of Primakoff-effect polarimeter is shown in Fig. 12.

The Primakoff-effect polarimeter is to detect an exclusive reaction that produces proton and π°. The detectors for the polarimeter include the forward spectrometer mentioned above and a lead-glass hodoscope as shown in Fig. 13. They accept the events which are in the region of the maximum analyzing power; $|t'| < 0.001$ (GeV/c)^2, $1.34 < M_{p\pi^\circ} < 1.50$ GeV/c^2, $70^\circ < \theta_{c.m.}^{\pi} < 120^\circ$, and $\Delta\phi = \pm 30^\circ$ on both sides of the beam line. The accuracy of the beam polarization can be expressed as $\Delta P = \frac{1}{A}\sqrt{\frac{1 - (PA)^2}{N}}$, where A is the analyzing power, P the beam polarization, and N the number of events.

Measurements of beam polarization at 200 GeV/c by this polarimeter were performed for several days in November 87 to January 1988. We were able to observe the Primakoff events in the $|t|$ region less than 10^{-3} (GeV/c)^2. Thus far, we have observed correct signs of beam polarization, which was detected

by the polarization and momentum tagging hodoscopes. Final results should be available soon.

II) First Round Experiments Using the Polarized-Beam Facility

Experiment 704, the Integrated Proposal on First Round Experiments with the Polarized Beam Facility, constitutes a proposal to simultaneously perform substantial parts of previously proposed Experiments # 674 (Asymmetries in Inclusive Pion and Kaon Production at Large x with a Polarized Beam), # 676 (An Experiment to Measure $\Delta\sigma_L$ in p-p and $\bar{p}$-p Scattering Between 100 and 500 GeV), # 677 (To Study the Spin Dependence in the Inclusive Production of Lambda Particles with the Polarized Beam), and # 678 (Proposal to Study the Spin Effects in Inclusive π^0 and Direct Gamma Production at High-$p_\perp$ with the Polarized Beam Facility).

Experimenters involved in these measurements are from Argonne National Laboratory, Fermi National Accelerator Laboratory, Kyoto University, Kyoto Sangyo University, Kyoto Education University, KEK (Tsukuba Japan), LAPP (Annecy, France), Los Alamos National Laboratory, Northwestern University, Rice University, CEN Saclay (France), IHEP-Serpukhov (USSR), University of Texas, and Trieste INFN (Italy).

The integrated proposal is for a 200-GeV/c conventional-magnet beam line. We will carry out the following measurements:

A) $\Delta\sigma_L(pp)$ and $\Delta\sigma_L(\bar{p}p)$

We intend to explore the spin dependence of the interactions in a global way using a straightforward experiment which will measure the difference in pp and $\bar{p}p$ total cross sections between the states with helicities of target and beam parallel and antiparallel.

$$\Delta\sigma^{Tot} = \sigma^{Tot}(\uparrow) - \sigma^{Tot}(\downarrow).$$

Experience shows that accuracy of $\pm$ 100 microbarns can easily be achieved.

Helicity asymmetries were found to be unexpectedly large at low energies and we are led to expect that they may persist into the region of Fermilab energies.

In $\bar{p}p$ interactions there are also good reasons to expect polarization effects at the highest energies. In any process at relativistic energy involving the annihilation of spin -1/2 particles into vector intermediate states, a reaction with initial particles having like helicities is almost completely suppressed (by a factor γ) relative to the rate for the same reaction in a state of opposite helicities.

The hodoscopes in this experiment are expected to be used for the polarimeter which measures transverse beam polarization through elastic scattering in the Coulomb-interference region. With a longitudinally polarized beam, the polarimeter cannot monitor the beam polarization directly during the actual experiment, and there is no conflict in using the same apparatus for both purposes. Beam polarization will be checked periodically by changing to transverse spin and inserting H_2 target or depolarizing the polarized target.

We will use a standard, longitudinally polarized proton target, in a superconducting solenoid target. A target material such as ethylene glycol or propanediol, 10% hydrogen by weight and with a free proton density of .07 gm/cm^3, can be used to reliably obtain polarizations above 80%.

Matrix logic will be used to reject multi-particle events, and other obviously inelastic or large-angle scattering events. For tracks that are nearly collinear, before and after the target, a hard-wired calculation of the scattering angle θ will be executed, and a corresponding scaler incremented.

Additional scalers will record the number of incident tracks and other pertinent matrix outputs. All scalers will be read into an on-line computer after each spill. In addition, magnet currents, target polarization, and hodoscope hit-patterns will be sampled periodically to monitor the data.

Beam passing through the polarized-proton target is attenuated by the the free polarized protons and the rest of the material. The number of particles, N_i (corrected for efficiency), transmitted through the target into the ith element of solid angle covered by segments of the transmission hodoscope is given by:

$$N_i^{\pm} = N_0^{\pm} \exp[-\alpha_i - \frac{1}{A} (\sigma_i \pm P_B P_T \frac{\Delta\sigma_{L,i}}{2})],$$

where $\pm$ refers to antiparallel (+) or parallel(-) beam and target polarizations, N_0 is the number of incident beam particles, α_i is the attenuation constant for everything in the target except free hydrogen, σ_i is the integrated differential cross section from the ith solid angle subtended, $A = (N_A \rho_F L)^{-1} =$ 2320 mb is the target constant for free hydrogen, N_A is Avogadro's number, $\rho_F = 0.0714$ g/cm^3 is the free-proton density, L = 10 cm is the target length, and $P_B = 0.45$ and $P_T = 0.8$ are the magnitude of the beam and target polarization, respectively.

The partial cross-section difference for each counter, $\Delta\sigma_{L,i}$, is calculated from these numbers by:

$$\tanh \frac{\Delta\sigma_{L,i} P_B P_T}{2A} = - \frac{N_i^+/N_0^+ - N_i^-/N_0^-}{N_i^+/N_0^+ + N_i^-/N_0^-} .$$

B) Hadron production on hydrogen target with polarized beam,

$p^{\uparrow}p \rightarrow (\pi^{\circ}, \pi^{\pm}, \Lambda^{\circ}, \Sigma^{\circ}) + X$

We will simultaneously study the inclusive production of neutral pions around $x_F \approx 0$ at large $p_{\perp}$, and of Λ°, Σ° at large x. We will measure single-spin asymmetries in the hadron production,

$$A_N = \frac{E\frac{d^3\sigma}{dp^3}\uparrow - E\frac{d^3\sigma}{dp^3}\downarrow}{E\frac{d^3\sigma}{dp^3}\uparrow + E\frac{d^3\sigma}{dp^3}\downarrow},$$

where the arrows refer to the transversity of the incoming proton.

Interpretation of the polarization of hyperons (Λ, Σ, Ξ) produced inclusively ($pp \rightarrow \Lambda^{\circ\uparrow}x$, $Kp \rightarrow \Lambda^{\circ\uparrow}x$, etc.) has given rise to extensive discussion about the origin of this polarization. We expect that information of spin transfer from initial to final state in this reaction will enlighten the debate.

The major detectors for this experiment are: i) two gamma spectrometers (called CEMC, central electromagnetic calorimeter), G1 and G2 as shown in Fig. 11, with 500 lead-glass cells each will be used to detect γ's from π° decay. Figure 14 shows the photograph of the CEMC in the experimental hall. ii) The magnetic spectrometer with proportional and drift-chamber systems (PC's and DC1 as shown in Fig. 11) and with a Cerenkov counter followed by lead-glass cells is to detect $\pi^{\pm}$, Λ°, and Σ°. Fast-electronics enclosures are placed along the various detectors as shown in Fig. 15.

The technique for measuring single spin measurements in hadron production is considerably improved over the previous experiment since the polarized beam allows the use of a liquid hydrogen target.

III) Second Round Experiments

During the first-round hadron production experiments, we will study the one-spin effect as mentioned above. As obvious follow-up experiment would be to measure the hadron production using the Polarized-Beam Facility and the Polarized Target Facility. We will measure the difference in the hadron production cross sections between the status with helicities of beam and target parallel and antiparallel.

$$p^{\uparrow}p^{\uparrow} \rightarrow (\pi^0, \pi^{\pm}, \Lambda^0, \Sigma^0) + X$$

While a perturbative QCD seems to have problems in predicting the polarization in the hadron production, it has a definite prediction for the hadron production at high $p_{\perp}$ in the pure helicity states.

For the spin-spin asymmetry measurements, we need to increase the angular acceptance of the detectors since the effective target polarization becomes much smaller than 80% mentioned above. For the pizero production measurement, we plan to double lead-glass cells in the CEMC.

IV) Future Experiments

Thus far, we have discussed large-$p_{\perp}$ π° and large-x hadron production measurements with polarized beams, since these channels are relatively easier to make measurements. We also would like to explore large-$p_{\perp}$ $\pi^{\pm}$, direct gamma production, and calorimeter triggered events.

Recently Brodsky, Ellis, and Karliner[11] suggested that most of the proton spin is due to gluons and/or orbital angular momentum and discussed various measurements to test this suggestion. Some of the experiments can be carried out with the Fermilab polarized beams. Direct experimental information on the

gluon polarization in a proton may be obtained in the measurements of $p^{\uparrow}p^{\uparrow} \rightarrow$ (Hadronic Jet or Direct photon) X at large $p_{\perp}$ [12] and $p^{\uparrow}p^{\uparrow} \rightarrow$ (hyperon) X at large $p_{\perp}$.[13] The interesting problem of how the spin of a hadron is shared among constituents may be tested in the proton-proton Drell-Yan process with polarized beam and target,

$p^{\uparrow}p^{\uparrow} \rightarrow (\ell^{+}\ell^{-})X$.[14]

Pending proposals using the Fermilab polarized-beam facility at the moment are proposed experiments #682 (Study of the $p_{\perp}$ Dependence of $\pi^{\pm}$ Inclusive Production with a Polarized Proton Beam and Target), #688 (Nuclear-Size Dependence of Single-Spin Asymmetries in High-p⊥ Hadron Production), and #699 (Study of Spin-Dependent Asymmetries Using Calorimeter Triggered High-$p_{\perp}$ Events with Polarized Beam and Polarized Target).

REFERENCES

1. O. Overseth, NAL 1969 Summer Study Report, SS-118, Vol. I.
2. J. W. Cronin and O. E. Overseth, Phys. Rev. 129 (1963) 1795; O. E. Overseth et al., Phys. Rev. Lett. 19 (1967) 391.
3. P. Dalpiaz et al., CERN/ECFA/72/4, Vol. I, p. 284; CERN proposal SPSC/p. 87, July 1977.
4. D. Underwood et al., A Polarized Beam for the M-3 Line (Fermilab), ANL-HEP-PR-78-05.
5. D. G. Underwood, Nucl. Inst. and Meth. 173 (1980) 351.
6. J. Schwinger, Phys. Rev. 73 (1948) 407.
7. For instance, C. Bourrely and J. Soffer, Nuovo Cimento Lett. 19 (1977) 569.
8. H. Primakoff, Phys. Rev. 81 (1951) 899; A. Halprin, C. M. Anderson, and H. Primakoff, Phys. Rev 152 (1966) 1295; L. Stodolsky, Phys. Rev. 144 (1966) 1145; G. Faldt, Nucl. Phys. B41 (1972) 125; B43 (1972) 591.
9. B. Margolis and G. H. Thomas, "High Energy Polarized Proton Beams", AIP Conference Proceedings, No. 42 (1978) p. 173.
10. D. G. Underwood, ANL-HEP-PR-77-56.
11. S. J. Brodsky, J. Ellis, and M. Karliner, SLAC-PUB-4519, January 1988.
12. M. B. Einhorn and J. Soffer, Nucl. Phys. 274 (1986) 714.
13. N. S. Craigie, V. Roberto, and D. Whould, Zeit. Phys. C12 (1982) 173.
14. E. Richter-Wgs and J. Szwed, Phys. Rev. D31 (1985) 633.

Figure Captions

Figure 1 Spin direction of protons vs. decay angles. The spin direction is indicated by => and $\hat{\parallel}$ symbols.

Figure 2 Virtual sources (top view).

Figure 3 Tevatron and MP beam line.

Figure 4 Top view of the Fermilab polarized beam (MP primary beam).

MP2TGT: parasitic target when MC beam line is on,

SWIC: segmented wire ionization chamber,

MP6SEM: secondary emission monitor,

MP6TGT: production target for the polarized beam

Figure 5 Side view of the Fermilab polarized beam (MP secondary beam).

Figure 6 Photograph of the snake magnets consisting of 12 dipoles located at the entrance to the experimental hall.

Figure 7 $\langle P \rangle$ vs. x in the tagging section.

Figure 8 $I\langle P \rangle^2$ (arbitrary unit) vs. x in the tagging section.

Figure 9 Comparison of estimated polarized beam intensity with 400- and 1000-GeV incident energies.

Figure 10 Proposed polarized beam upgrade. The dashed and solid curves refer to total flux/spill and flux with 45% polarization, respectively.

Figure 11 Detectors in the MP experimental hall (top view).

HB1,2,3,: beam hodoscope, HB4,5,6: transmission hodoscope, Target: polarized proton target/hydrogen target/polarimeter target, H1 to H4: trigger hodoscope, MSD1,2: multistrip solid-state detector, PC1 to 14: MWPC, V1, V2: veto hodoscope, G1,2: lead-glass calorimeter, G3,4: lead-glass hodoscope.

Figure 12 Primakoff effect.

Figure 13 Photograph of the Primakoff polarimeter placed upstream of the analyzing magnet, BM-109.

Figure 14 Photograph of the CEMC (Central Electromagnetic Calorimeter).

Figure 15 Photograph of the fast-electronic enclosures.

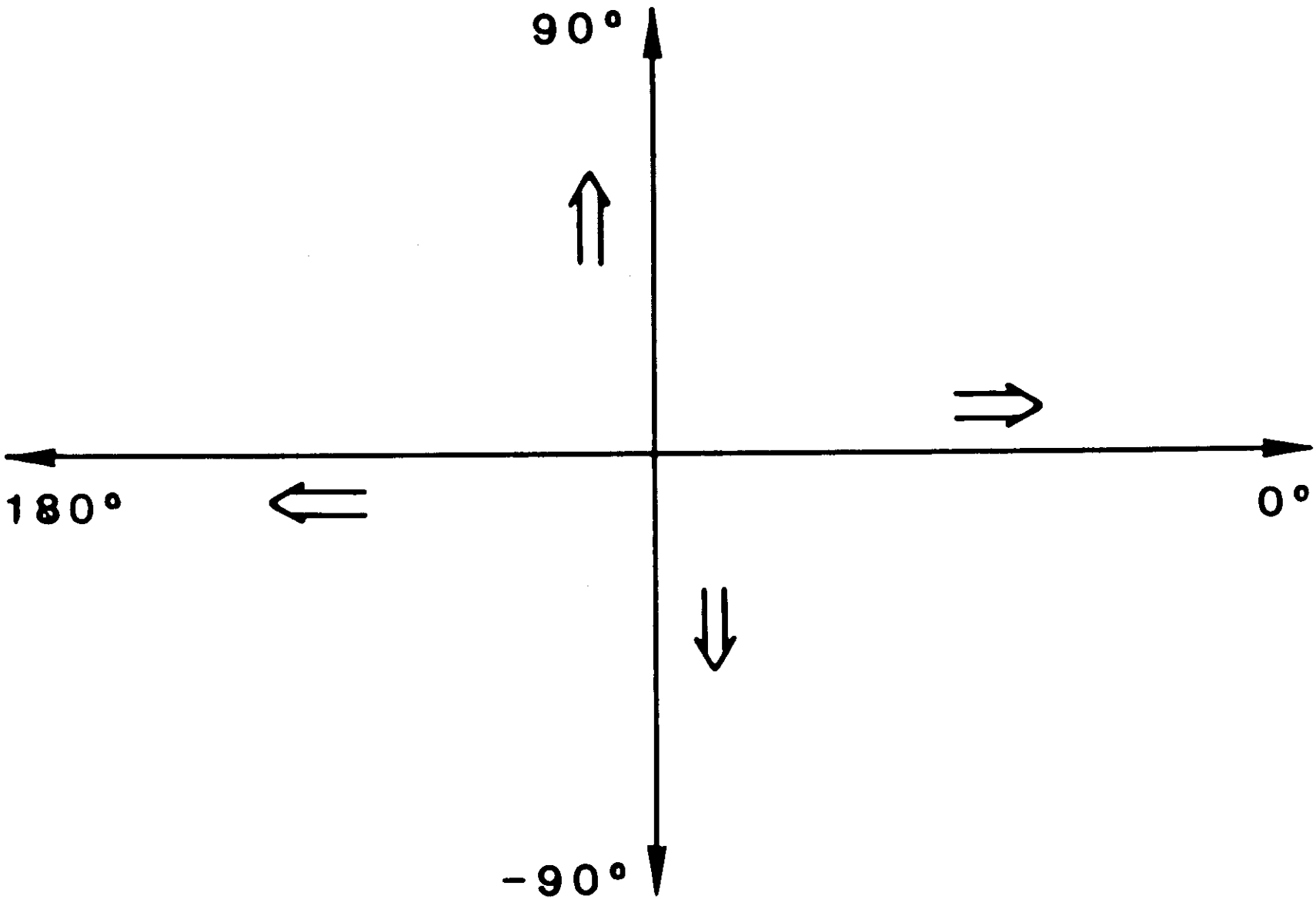

Figure 1

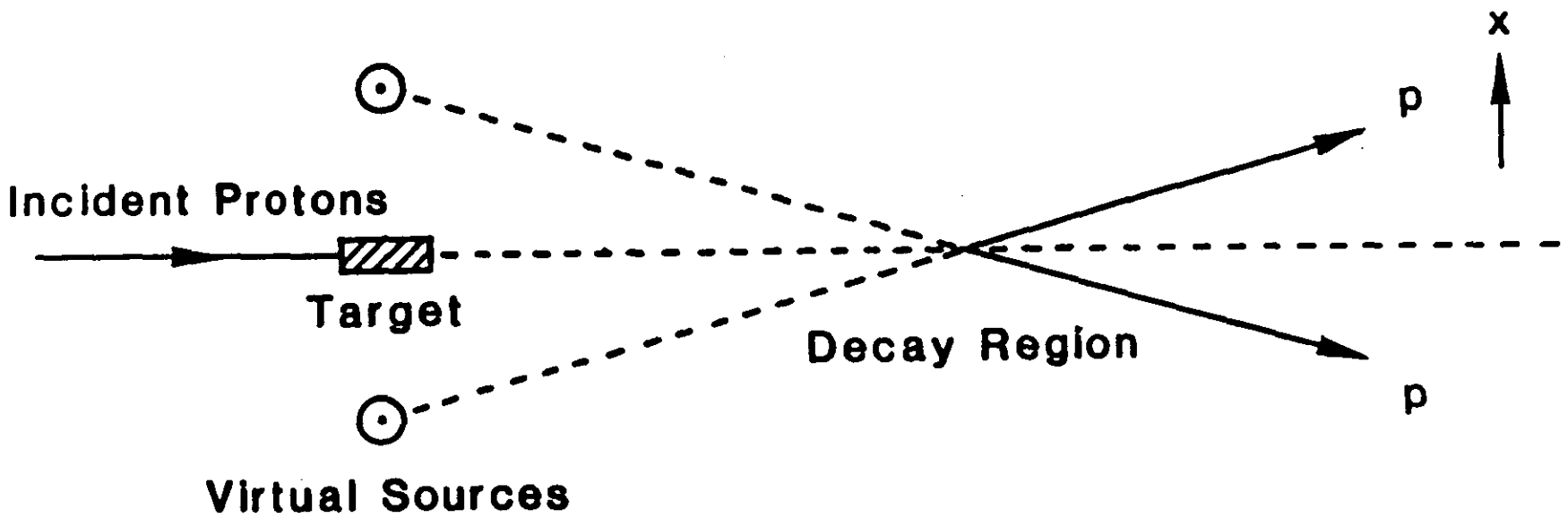

Figure 2

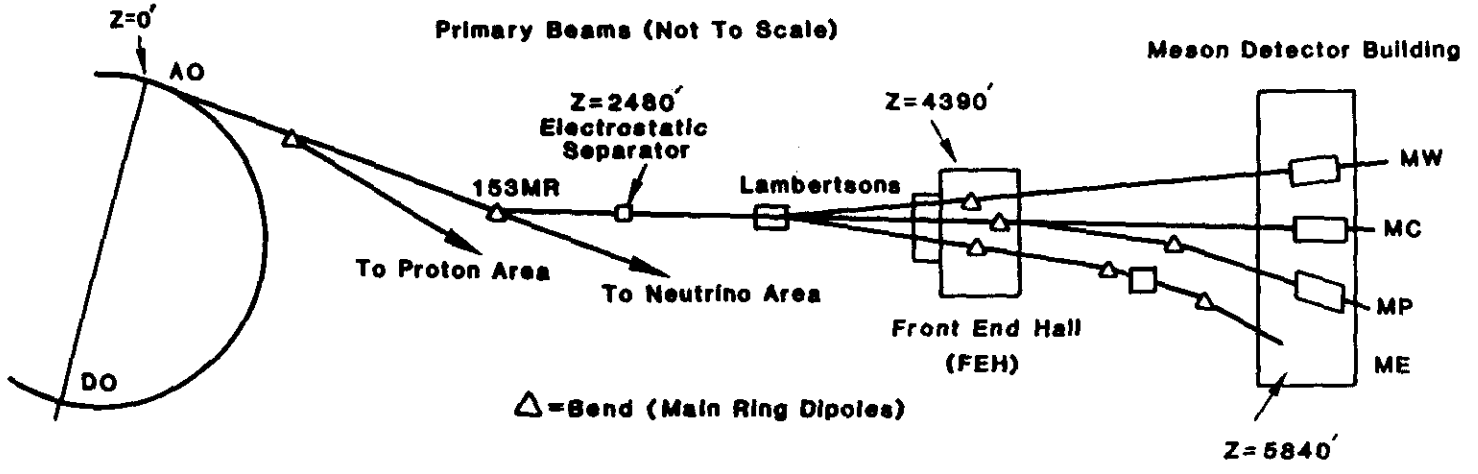
Z=0′
AO
DO
Primary Beams (Not To Scale)
Z=2480′
Electrostatic
Separator
153MR
To Proton Area
To Neutrino Area
Lambertsons
Z=4390′
Front End Hall
(FEH)
Meson Detector Building
MW
MC
MP
ME
Z=5840′
△=Bend (Main Ring Dipoles)

Figure 3

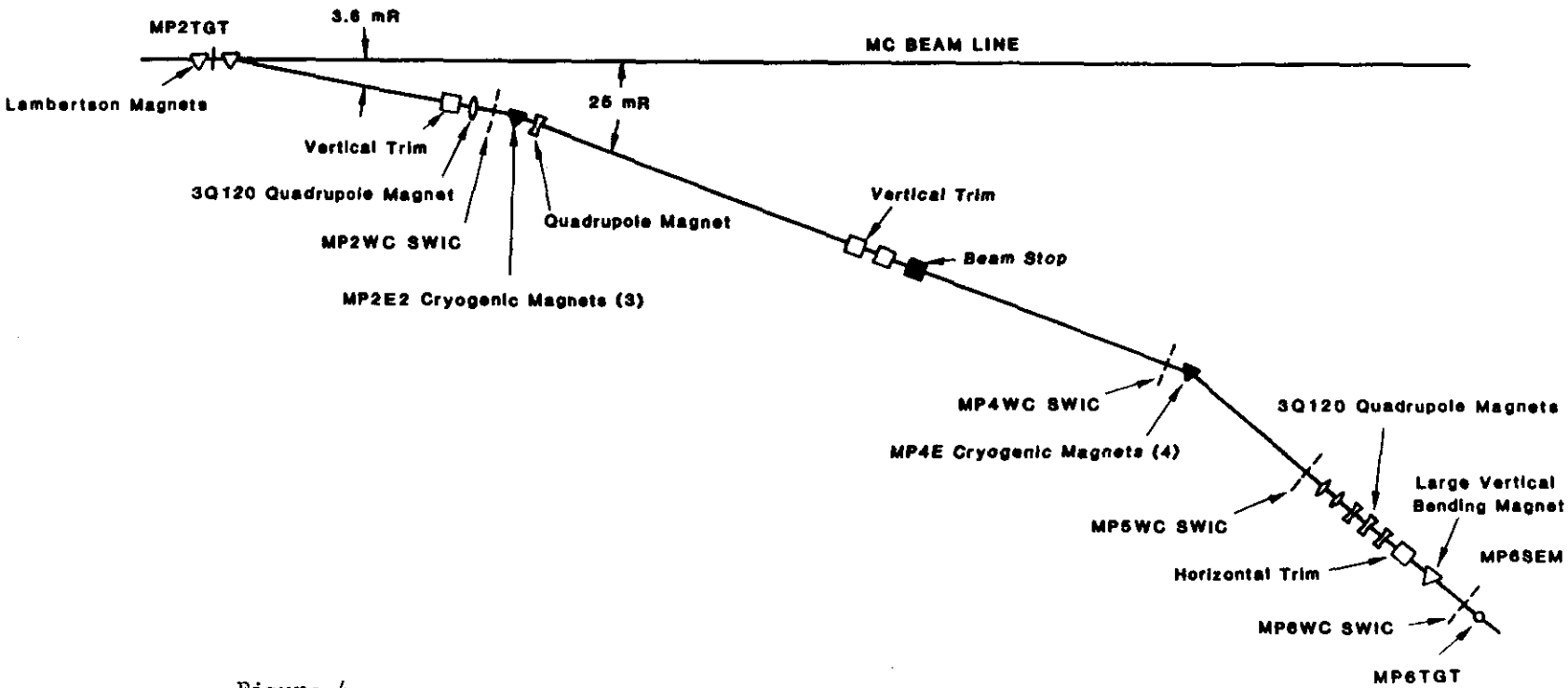
MP2TGT
3.6 mR
MC BEAM LINE
Lambertson Magnets
25 mR
Vertical Trim
3Q120 Quadrupole Magnet
MP2WC SWIC
Quadrupole Magnet
MP2E2 Cryogenic Magnets (3)
Vertical Trim
Beam Stop
MP4WC SWIC
MP4E Cryogenic Magnets (4)
3Q120 Quadrupole Magnets
Large Vertical
Bending Magnet
MP5WC SWIC
MP6SEM
Horizontal Trim
MP6WC SWIC
MP6TGT

Figure 4

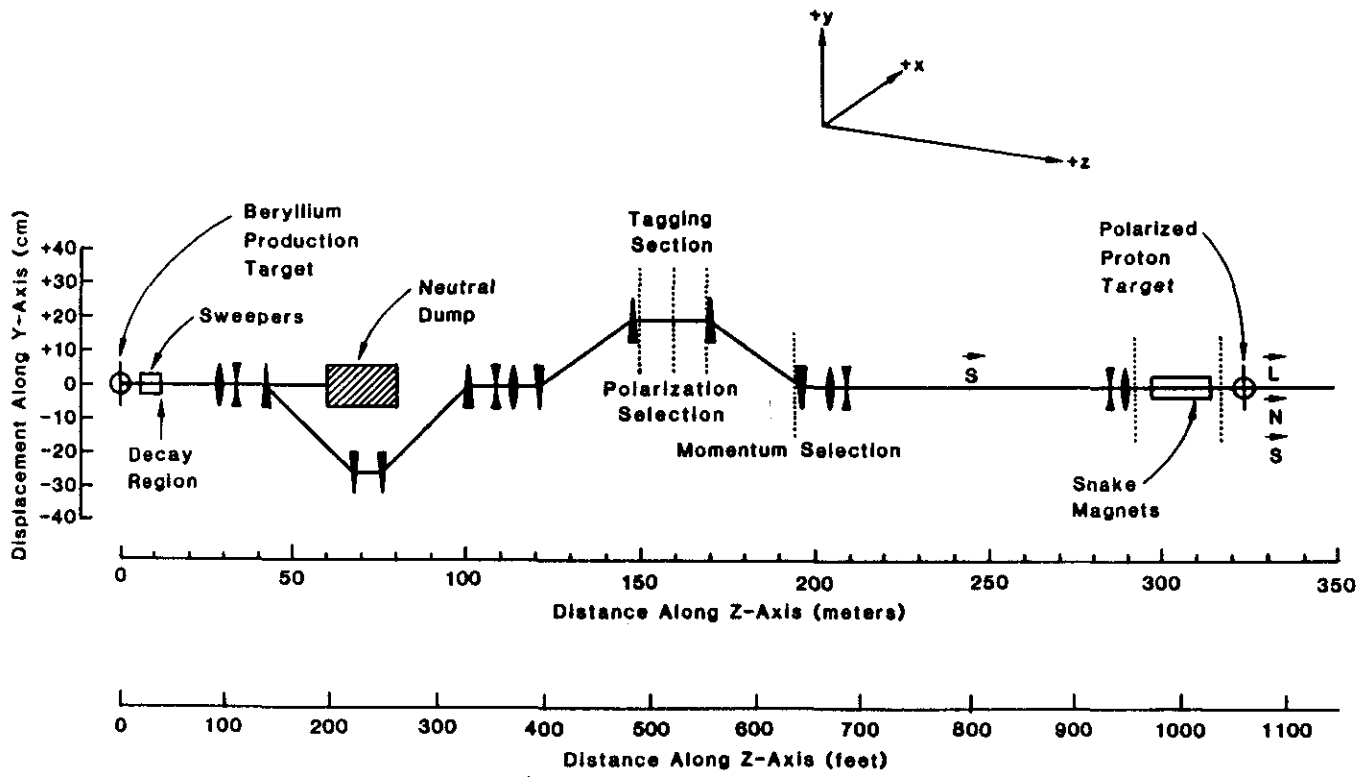
+y
+x
+z
Beryllium
Production
Target
Sweepers
Neutral
Dump
Tagging
Section
Polarized
Proton
Target
Polarization
Selection
Momentum Selection
S
L
N
S
Decay
Region
Snake
Magnets
Displacement Along Y-Axis (cm)
+40
+30
+20
+10
0
-10
-20
-30
-40
0
50
100
150
200
250
300
350
Distance Along Z-Axis (meters)
0
100
200
300
400
500
600
700
800
900
1000
1100
Distance Along Z-Axis (feet)

Figure 5

Figure 6

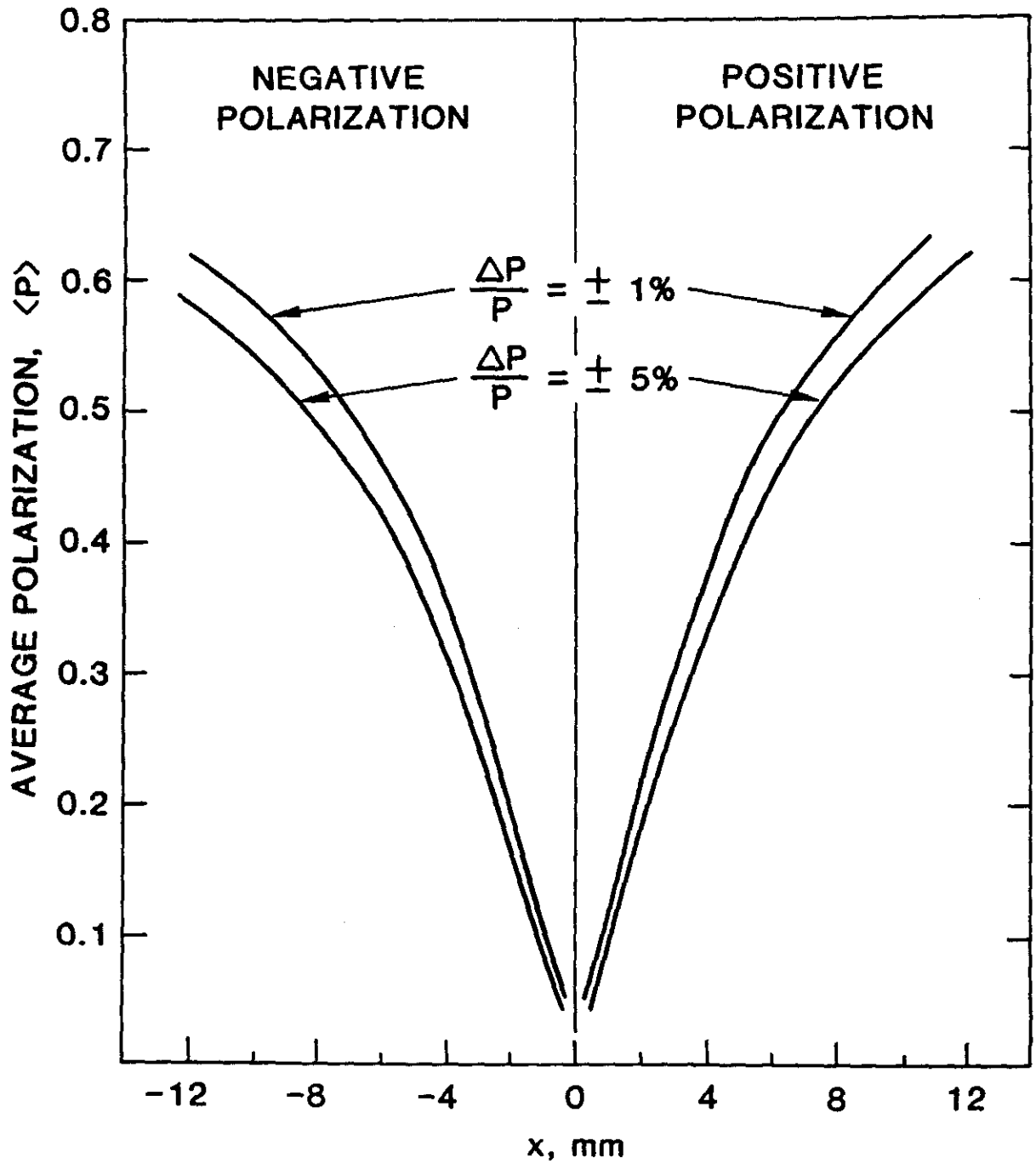
NEGATIVE POLARIZATION
POSITIVE POLARIZATION
ΔP/P = ± 1%
ΔP/P = ± 5%
AVERAGE POLARIZATION, ⟨P⟩
0.8
0.7
0.6
0.5
0.4
0.3
0.2
0.1
-12
-8
-4
0
4
8
12
x, mm

Figure 7

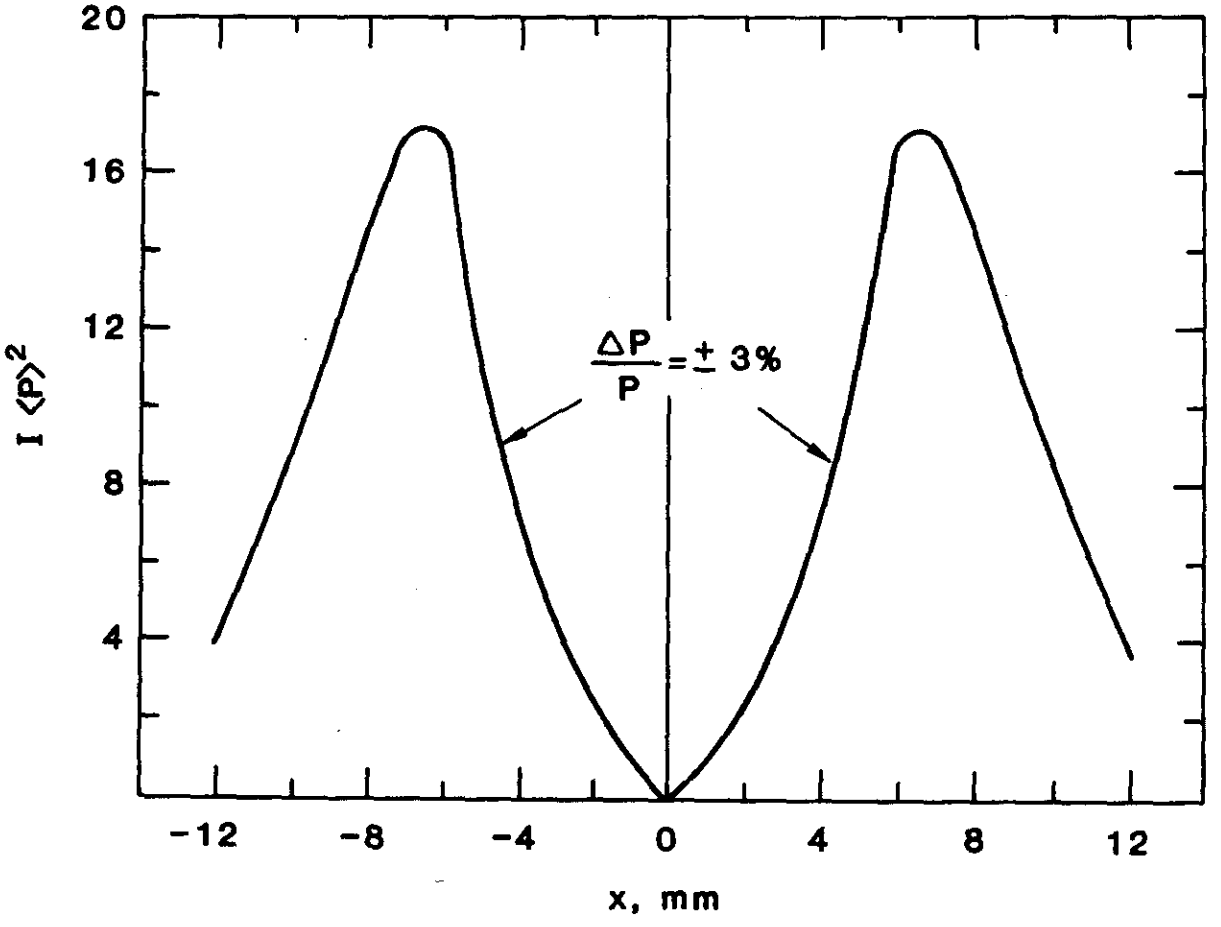

Figure 8

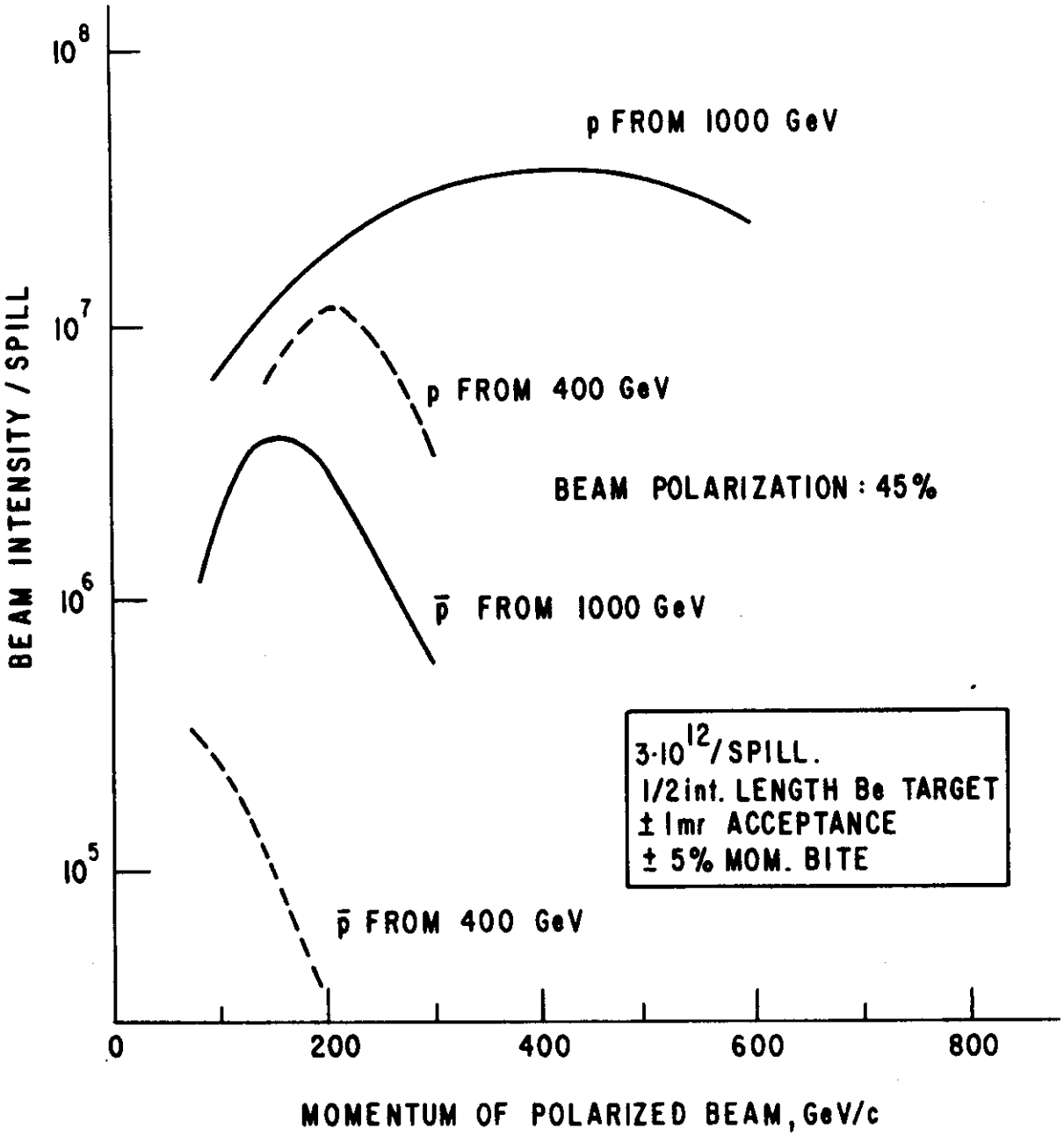
BEAM INTENSITY / SPILL
10^8
10^7
10^6
10^5
p FROM 1000 GeV
p FROM 400 GeV
BEAM POLARIZATION : 45%
$\bar{p}$ FROM 1000 GeV
$3 \cdot 10^{12}$/SPILL.
1/2int. LENGTH Be TARGET
± 1mr ACCEPTANCE
± 5% MOM. BITE
$\bar{p}$ FROM 400 GeV
0
200
400
600
800
MOMENTUM OF POLARIZED BEAM, GeV/c

Figure 9

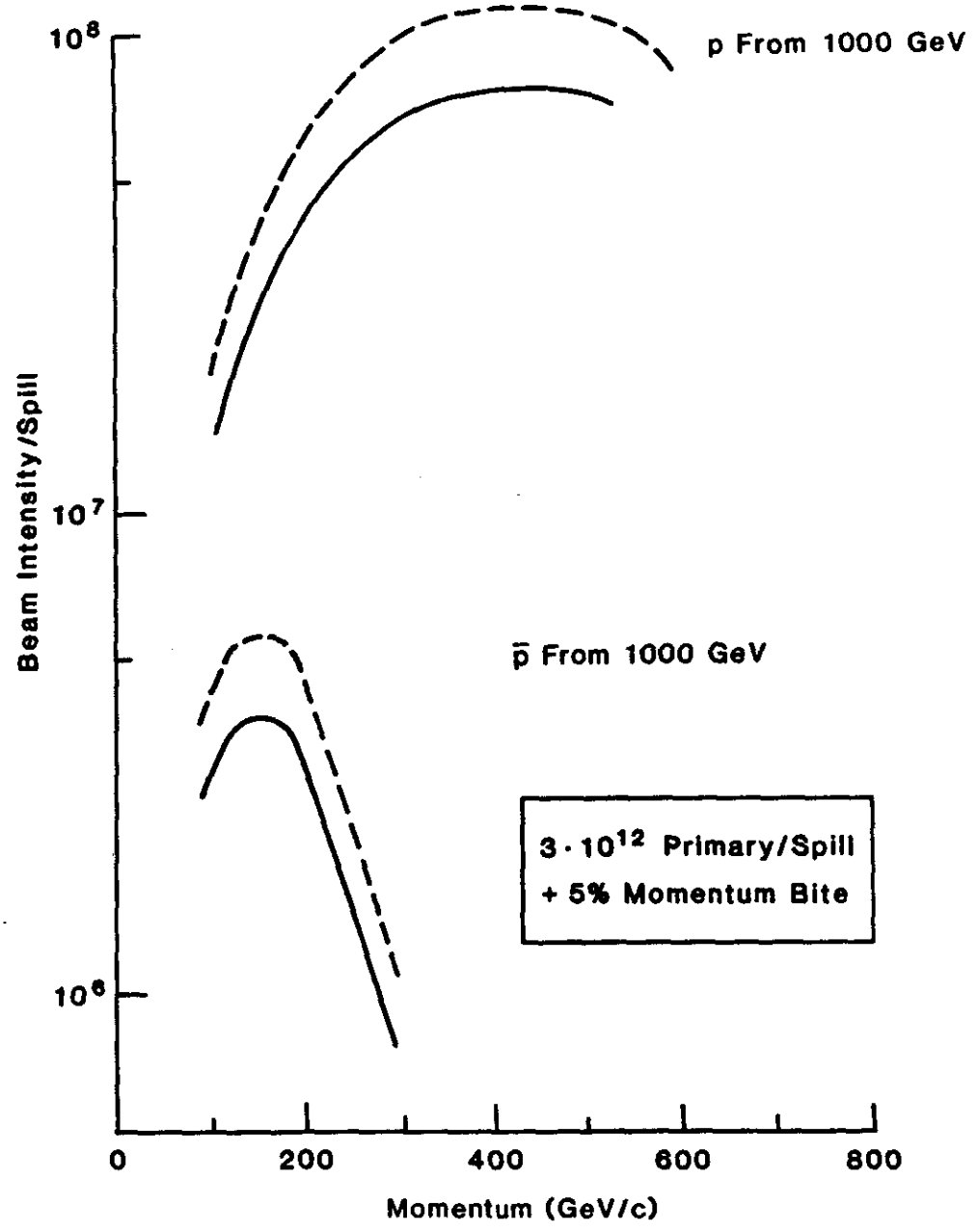
p From 1000 GeV
p̄ From 1000 GeV
3 · 10^12 Primary/Spill
+ 5% Momentum Bite
Beam Intensity/Spill
10^8
10^7
10^6
0
200
400
600
800
Momentum (GeV/c)

Figure 10

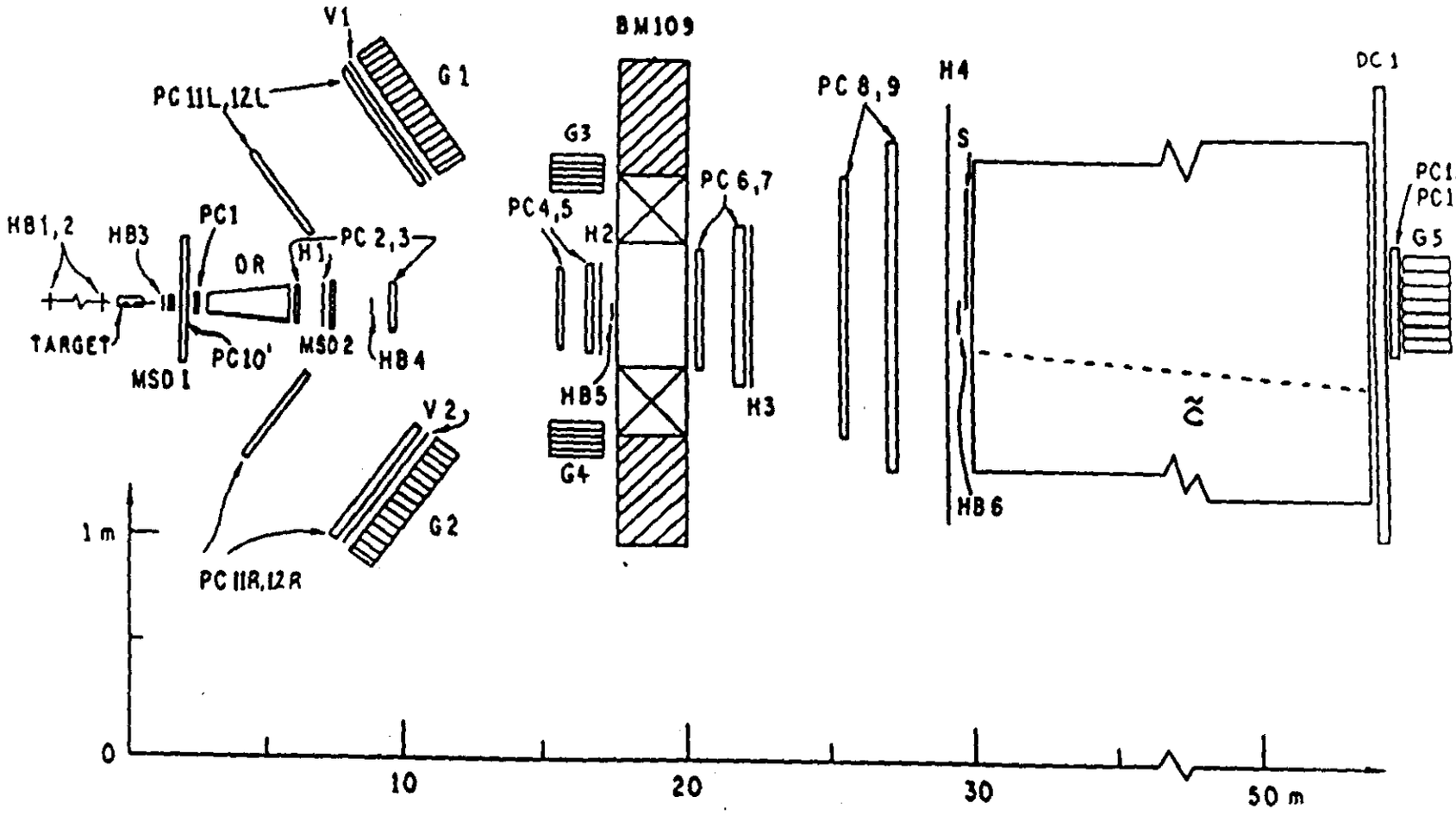
V1
G1
PC 11L,12L
BM109
G3
PC 8,9
H4
DC 1
S
PC 6,7
PC13
PC14
PC4,5
H2
G5
HB1,2
HB3
PC1
DR
H1
PC 2,3
TARGET
PC10'
MSD 2
HB4
MSD 1
HB5
H3
V2
G4
HB6
1 m
G2
PC 11R,12R
0
10
20
30
50 m

Figure 11

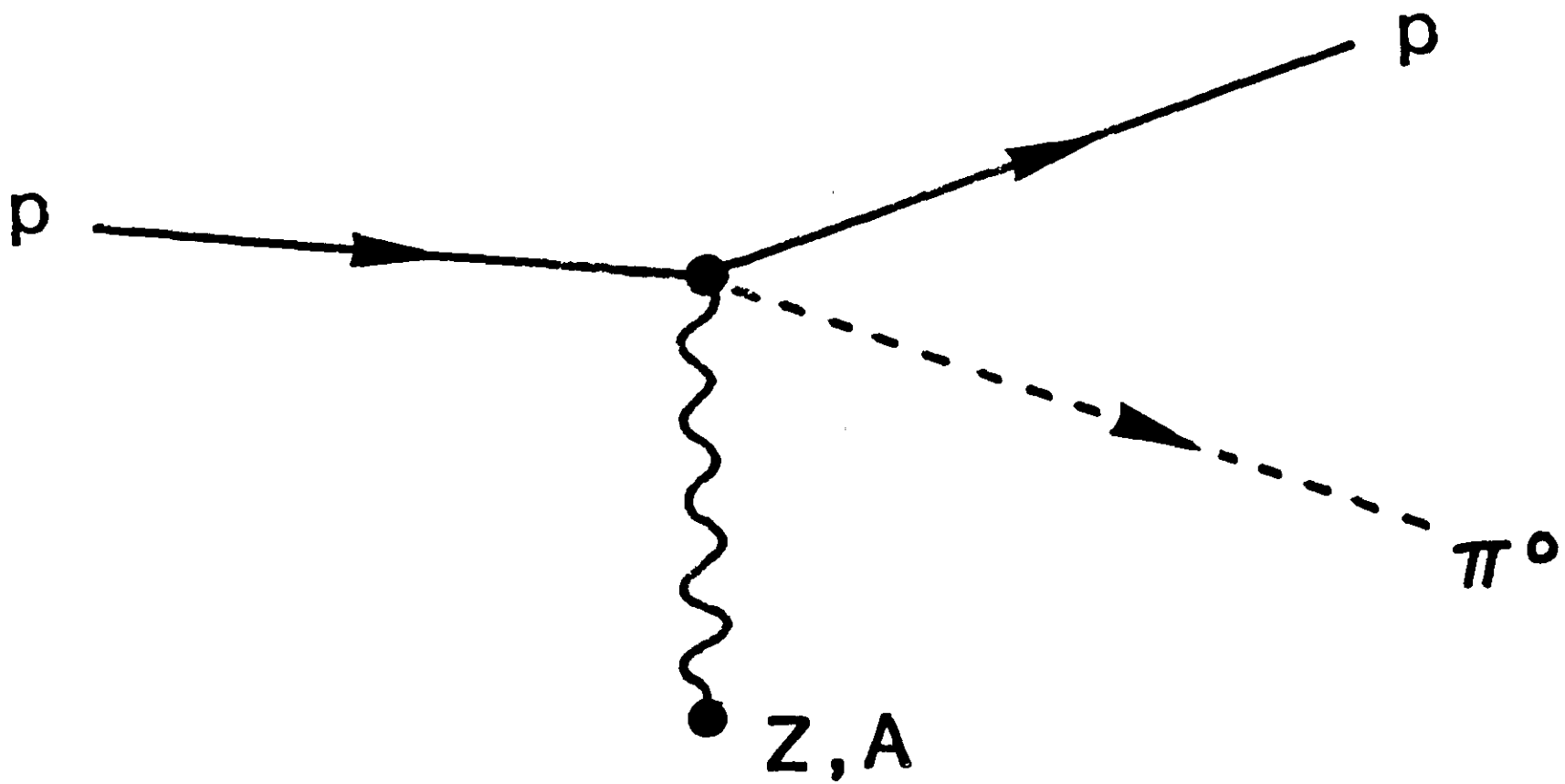

Figure 12

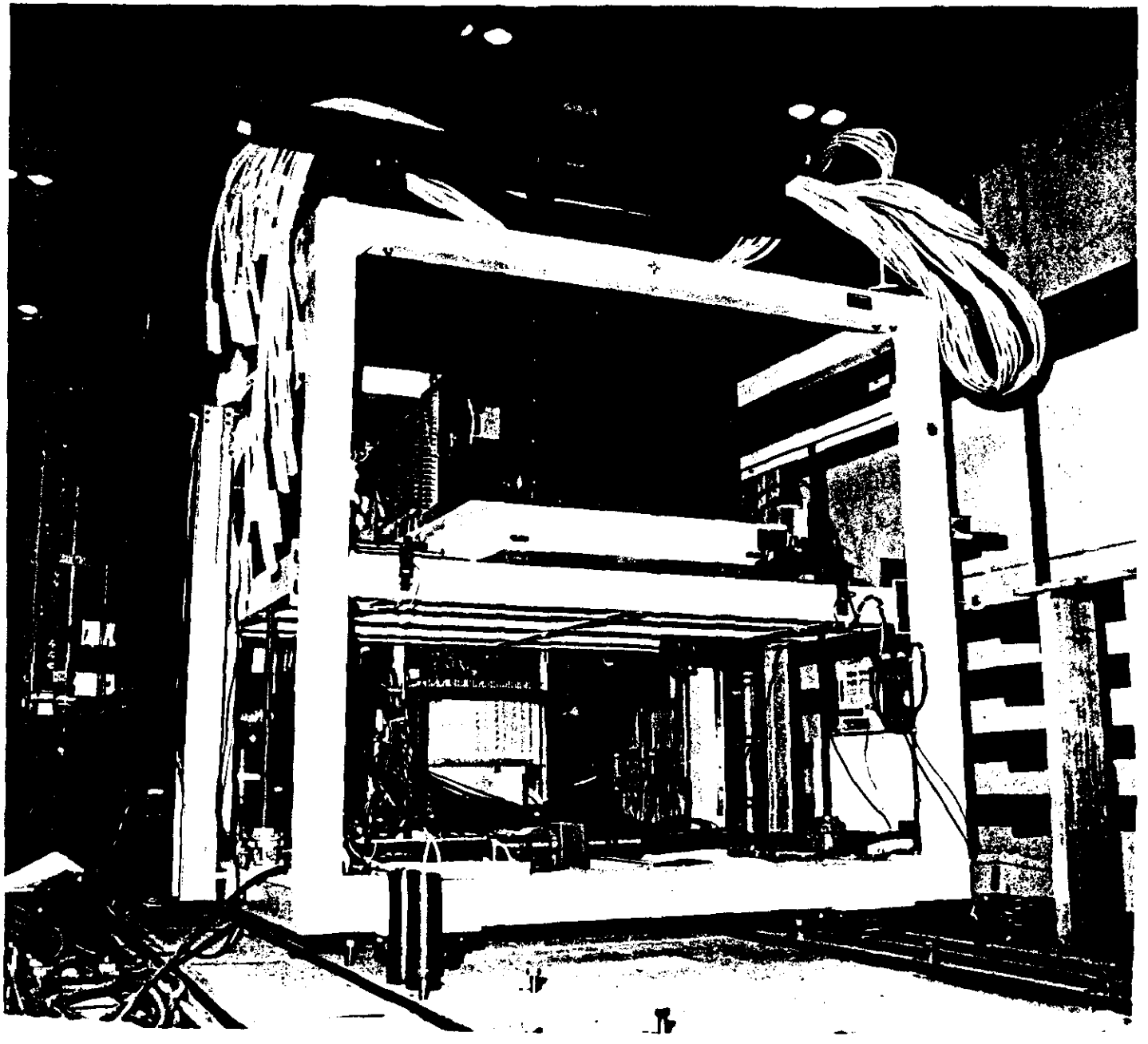

Figure 13

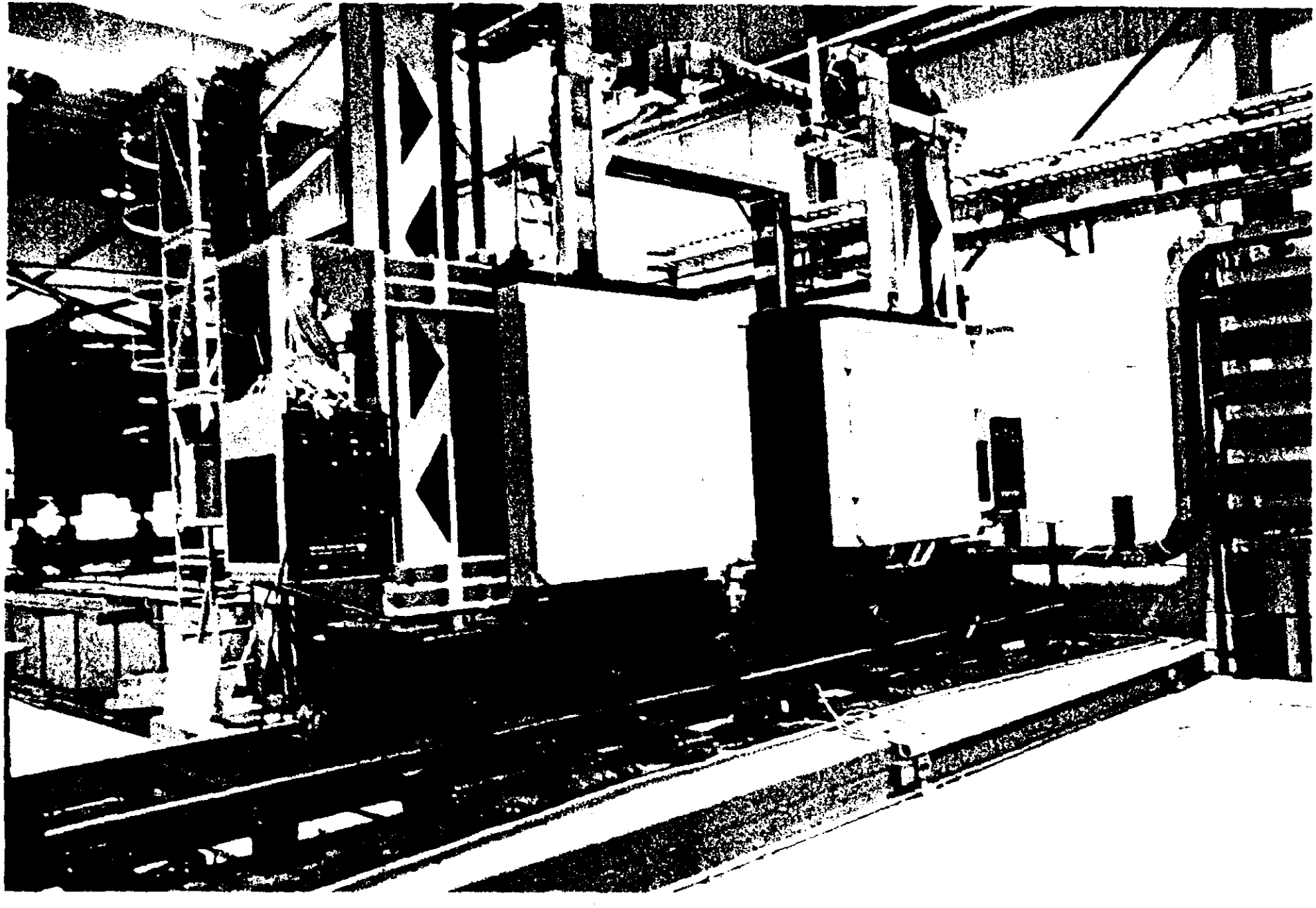

Figure 14

Figure 15